



## Supplementary Materials for

### Flower Discrimination by Pollinators in a Dynamic Chemical Environment

Jeffrey A. Riffell, Eli Shlizerman, Elischa Sanders, Leif Abrell, Billie Medina,  
Armin J. Hinterwirth, and J. Nathan Kutz

\*Correspondence to: [jriffell@uw.edu](mailto:jriffell@uw.edu)

**This PDF file includes:**

Materials and Methods  
Figs. S1 to S12  
Tables S1 to S3  
References 23-47

**Other Supplementary Material for this manuscript includes the following:**

Database S1

## MATERIALS AND METHODS

### Flower volatile sampling

*Field site:* *Datura wrightii* (hereafter: *Datura*) flower volatiles were sampled at the Santa Rita Experimental Range (SRER), approximately 60 km north of the US/Mexico border. At this field site, *Datura* plants were at low densities (approximately 0.004 plants/m<sup>2</sup>), and patchily distributed (10, 23). By contrast, *Larrea tridentata* (hereafter: creosote bush) is the dominant vegetation species at this study site at the northern boundary of the SRER (31°54044.2600 N, 110°50012.9200 W, 994 m a.s.l.). At this location, creosote bush dominates the total canopy cover, comprising approximately 50 to 60% of the vegetative canopy (24) and can be found in close proximity to *Datura* plants (distances from the focal *Datura* plants in this study are 0.76 ± 1.17 m). Creosote bush emits a high levels of volatiles in the environment, particularly during the monsoon season of the summer months (80.4 µg C/gdw/h), and is often referred to in Sonora, Mexico as hediondilla, the “little stinker”. Although creosote bush emissions have a diurnal peak, nocturnal emissions remain strong over the course of the evening (eg, methyl ethyl ketone emissions drop approximately 15% at 12am versus 12pm). The headspace of creosote bush is a complex mixture of oxygenated volatiles, including aromatics, terpenes, and aliphatics, and includes the oxygenated aromatic compound, benzaldehyde (12), also found in the *Datura* headspace and an important volatile in attracting moths to the flowers (13).

*Proton Transfer Reaction - Mass Spectrometry and Gas Chromatography – Mass Spectrometry:* PTR-MS has been used extensively to measure the concentrations of atmospheric volatile organic compounds, and technical details of the PTR-MS have been previously described (25, 26). Flower volatiles were measured using a commercial high sensitivity PTR-MS instrument (IONICON, Austria, with a QMZ 422 quadrupole mass spectrometer, Balzers, Switzerland). Most of the *Datura* volatiles identified by GC-MS were measured by PTR-MS as protonated parent ions produced in the drift tube with a 0.5 s dwell time. Inside the PTR-MS H<sub>3</sub>O<sup>+</sup> ions (*m/z* 21) transferred a proton to compounds in the sample air. All chemical species must be protonated to be visible by the analyzer and ion counter. Protonated monoterpenes (eg, linalool, ocimene), oxygenated aromatics (benzaldehyde, benzyl alcohol), and sesquiterpenes (caryophyllene) were detected by the mass spectrometer as its molecular mass plus one (27). These select compounds were analyzed concurrently, allowing for high temporal distinction between successive measurements. It should be noted, however, that these target ions might be also fragments from other, non-target, compounds. To properly characterize our samples, at the beginning of the experiment two methods were used to calibrate the PTR-MS. In the first method, a single calibration was performed with the monoterpene,  $\alpha$ -pinene, at a final concentration of 28 ppb, was placed in the permeation tube and sampled by the PTR-MS. In a second method, a mixture of volatiles – including benzaldehyde, methyl salicylate, acetone, and isoprene, all diluted in cyclohexane –, were injected into an enclosed Tevlar bag and sampled by the PTR-MS. Normalized sensitivities for  $\alpha$ -pinene using a permeation tube method were in close agreement with the Tevlar bag method, suggesting that cyclohexane solutions were a repeatable and accurate method for calibration of the PTR-MS. Most of the *Datura* compounds identified by GC-MS (described below) were also measured by PTR-MS as protonated parent

ions. However, a fragment at  $m/z$  136 was also used to monitor both hydrocarbon (eg, E- $\beta$ -ocimene) and oxygenated (eg,  $\pm$ linalool) monoterpenoids to increase the signal resolution at the short dwell times of 20 to 500 ms. Continuous ambient concentration measurements were carried out five times during the CREosote ATmosphere Interactions through Volatile Emissions (CREATIVE 2009) field study that occurred between June 10 to October 1 2009. The raw VOC signal intensities (counts per second [cps]) were normalized by the primary ion signal (cps<sub>21</sub>) and two minute averages were calculated at each sampling location (0, 0.1, 0.5, and 2.5 m) downwind of the *Datura* flower. Based on these measurements, conditional fluctuation statistics (e.g., statistics conditioned to include contributions only when the plume concentration was non-zero) were determined, including the odor filament frequency (Hz) and intermittency (% of the time the concentrations were non-zero). Simultaneously with the PTRMS measurements, a 3D sonic anemometer (Young 81000; RM Young Co., Traverse City, MI USA) was used to characterize the aerodynamic conditions during the sampling effort. The anemometer was placed 1 m from the PTRMS and transverse to the mean wind direction to minimize turbulent fluctuations in the VOC measurements. From the anemometer measurements, median wind velocities, turbulent intensities and Reynolds stresses were determined. Sampling began after 6 pm at which time *Manduca sexta* (hereafter: *Manduca*) begins to forage and the turbulent wind intensities are 4 to 90-times lower than daytime conditions (4). During a sampling effort, mean turbulent intensities at each location were not significantly different from one another (one-way ANOVA:  $F_{5,35} = 1.44$ ,  $P = 0.23$ ).

In addition to sampling the *Datura* and creosote bush volatiles with the PTR-MS, emissions were also analyzed using dynamic headspace sorption methods and run on a Gas Chromatograph with Mass Spectrometric detection (GCMS) (10, 28). This method allowed identification of the headspace volatiles from both odor sources. Briefly, *D. wrightii* flowers or branches of the creosote bush were enclosed in Teflon bags cinched at 500 mL volumes with plastic ties. Portable diaphragm pumps (10D1125, Gast Manufacturing Inc., Benton Harbor, MI, USA) were used to pull fragrant headspace air through sorbent cartridge traps (50 mg of Poropak Q adsorbent (mesh size 80–100)) at a flow rate of 1 L/min. Scent collections began at sunset and continued overnight for 12 h. Trapped volatiles were eluted from sorbent cartridges using 600  $\mu$ L of HPLC-grade hexane, and subsequently analyzed using GCMS, consisting of an HP 7890A GC and a 5975C Network Mass Selective Detector (Agilent Technologies, Palo Alto, CA, USA), with the inlet temperature set to 220 °C. A DB5 GC column (J&W Scientific, Folsom, CA, USA; 30m, 0.25mm, 0.25 $\mu$ m) was used, and helium was used as carrier gas at constant flow of 1cc/min. The initial oven temperature was 50 °C for 5 min, followed by a heating gradient of 10 C/min to 250 °C, which was held isothermally for 10 min. Chromatogram peaks were identified tentatively with the aid of the NIST mass spectral library (ca, 120,000 spectra), published Kovats Indices, and verified by chromatography with authentic standards (when available).

### Moth rearing

Naïve *Manduca* (Lepidoptera: Sphingidae) larvae were obtained from the *Manduca*-rearing facility of the Department of Biology of the University of Washington, Seattle. Larvae were reared on artificial diet (modified from (29)) supplemented with cholesterol (5 g), wheatgerm (144 g; 0.5 mg carotenoids), cornmeal (140 g; 2 mg carotenoids), soy (76 g; 10 mg carotenoids), linseed oil (9 mL), and sugar (36 g) to enhance adult vision. Larvae were reared under long-day

light:dark (LD) regimen (LD 17:7) at 25–26 °C and 40–50% relative humidity (RH). Pupae were segregated by sex and held in a rearing room under reverse-photoperiod conditions (LD 14:10) and with a superimposed temperature cycle: LD 26:24 °C. Three days before adult eclosion, male pupae were transferred to fiberglass-screen cages (31×31×32 cm) under 75-85% RH and ambient light conditions.

### Wind tunnel behavioral experiments

*Wind tunnel and stimuli:* A Plexiglas wind tunnel (L x W x H = 2.5 x 1 x 1 m) was used to create a highly controlled wind flow environment for examining upwind flight behavior in response to *Datura* odor plumes (Fig. S1). The wind-tunnel conditions were physicochemically scaled to match the odor emission rate equivalent to that of the *Datura* flower and creosote bush emissions, and the filament frequencies used in physiological experiments. Longitudinal (u) wind speeds in experiments were 50 cm/s. At the beginning of scotophase, naïve, adult male moths were placed individually 2 m downwind from the odor source. Each moth was allowed to fly freely inside the wind tunnel for 3 min, during which its behavior was recorded. Two types of behavioral data were acquired during experiments: (1) 3-dimensional video acquisition and motion analysis of moth flight behavior for each treatment group, and (2) scoring of moth behaviors. Scored behaviors were: wing fanning (typical behavior just prior to flight), upwind flight (moth comes within 0.75 m of odor source), close hover (moth hovered within 10 cm of odor source), source contact, and proboscis extension into the flower corolla (hereafter termed “feeding”). The scored categorical variables were analyzed by means of a 2-by-2  $\chi^2$ -test when comparing pairs of proportions. An  $\alpha$ -level of significance of 0.05 was used. Olfactory stimuli used in these experiments included a 3-component mixture of benzyl alcohol (13  $\mu\text{g}/\mu\text{l}$ ; 99.5% purity, Sigma-Aldrich), benzaldehyde (0.5  $\mu\text{g}/\mu\text{l}$ ;  $\geq 99.5\%$  purity, Aldrich), and ( $\pm$ )linalool (1  $\mu\text{g}/\mu\text{l}$ ;  $\geq 99\%$  purity, Fluka) that is sufficient and necessary for mimicking the natural floral scent of the *Datura* flower containing approximately 60-80 volatiles (9, 10, 30). The 3-component mixture (hereafter, *Datura* odor) evokes the same behavior and electrophysiological responses as the natural *Datura* scent (13, 30), but provides a less complex alternative that potentially activates fewer olfactory channels – by being composed of 3 volatiles – at the antennal and AL levels. In addition, background volatiles were tested, including benzaldehyde (10  $\mu\text{g}/\mu\text{l}$ ); geraniol (10  $\mu\text{g}/\mu\text{l}$ ; 98% purity, Aldrich); and ethyl sorbate (10  $\mu\text{g}/\mu\text{l}$ ; 98% purity, Aldrich). These three volatiles were tested because they offer a decreasing similarity to components in the *Datura* odor, and thus decreasing ability to alter the balance of excitation and inhibition in the moth AL: benzaldehyde is also in the *Datura* odor and creosote bush scent, and when presented as a background could potentially alter the balance of excitation and inhibition in the system; geraniol is a volatile that is not necessary for moths ability to recognize the *Datura* odor, but it is also found in the natural *Datura* scent, elicits strong AL neural responses, and is structurally similar to linalool and thus may potentially activate the olfactory channels as linalool; last, ethyl sorbate is not found in either the *Datura* or creosote bush scents and thus offers a background that is unique to the *Datura* odor (10). Intensities of background volatiles reflect the natural intensities in the environment (12, 13).

In addition to the single volatiles used above, we also tested the aromatic volatiles toluene ( $\geq 99.5\%$  purity, Sigma-Aldrich) and *p*-xylene ( $\geq 99.5\%$  purity, Fluka). The volatiles are structurally similar to benzaldehyde and benzyl alcohol, and are naturally emitted from forest fires and also are major constituents in vehicle exhaust emissions (1, 2, 22). For behavioral and electrophysiological experiments, we used three different concentrations: 100 ng/ $\mu$ l (High, [H]), 10 ng/ $\mu$ l (Medium, [M]) and 1 ng/ $\mu$ l (Low, [L]) that corresponded to mean intensities of 4059 ppb ( $\pm 1100$  SD), 118 ppb ( $\pm 10$  SD), and 2.3 ppb ( $\pm 0.5$  SD), respectively (for details on quantification method, see below). Volatile intensities of toluene and other aromatics can be low in remote areas ( $< 0.1$  ppb), but can be orders of magnitude higher in suburban and urban areas (0.8 and 9.8 ppb, respectively). Moreover, studies have quantified toluene intensities ranging from 0.08 to 2.54 ppb (2, 31), 0.92 to 38.49 ppb (32-35), and 5.5 to 568.7 ppb (34, 36, 37) in rural, urban and source dominated environments, respectively.

Mixtures were also tested as background, including the natural creosote bush scent (a positive background control). The creosote bush background allowed for testing how a complex mixture, but one that also included benzaldehyde, modified moth tracking behavior. We additionally tested the *Datura* odor as a background, which allowed for examining whether the moth could track the plume when the entire wind tunnel was saturated with the odor. Results from the latter test produced similar levels of behavior as the no-odor (mineral oil) control (38% responses from 21 male moths;  $2 \times 2$   $\chi^2$ -test comparing the uniform *Datura* odor with the control:  $P = 0.30$ ).

Lastly, the single volatile backgrounds were also individually tested alone without the *Datura* odor plume, and a mineral oil (no odor) control was tested as a negative control (20-50 moths tested per stimulus). Results from these experiments showed that moths responded similarly to the single background volatiles as to the no-odor (mineral oil) control (approximately 25% responses to the different volatile backgrounds from 60 total moths;  $2 \times 2$   $\chi^2$ -test comparing the single volatile backgrounds with the control:  $P = 0.76$ ).

To ensure proper scaling between electrophysiological and wind tunnel experiments, and to quantify stimulus emissions relative to those in the environment, we used solid-phase microextraction fibers (SPME; 75  $\mu$ m Carboxen/PDMS; Supelco, Bellefonte, PA USA). SPME is a rapid and sensitive pre-concentration method for sampling VOCs in air (38, 39). To quantify the SPME samples, gas samples were first created from a calibrated gas standard (100 ppm in  $N_2$ ; Cross Instrumentation, Conyers, GA USA). Samples were prepared and diluted in  $N_2$  gas using Bronkhorst High-Tech mass flow controllers (IQF-200C; Bronkhorst USA Inc., Bethlehem PA USA) to create final concentrations ranging from 0.1 to 10,000 ppb. SPME fibers were exposed for 60 to 180 min. and then run on the GCMS using the same conditions as described above (Fig. S2). A preliminary experiment using concentrations of 0.1 to 100 ppb showed that the sorption process did not reach equilibrium state at these exposure times. Three to five replicates were carried out for each of the calibration levels and the blanks.

*Experimental series:* Five different experimental series were conducted in the wind tunnel (742 total moths tested). The first experimental series examined the moth's ability to follow odor pulses at different frequencies; the second series examined the effects of a background odor, or volatile, on the moth's ability to track the *Datura* odor; the third series examined the effects of background volatiles that are both anthropogenic in origin and naturally-emitted from forest fires; the fourth series examined how prolonged exposure to background odors influenced

behavior; and the fifth series examined how inhibition in the moth antennal lobe influenced the ability for the moth to track the *Datura* odor.

The first experimental series examined the moth's ability to follow odor pulses at different frequencies. The *Datura* odor was pulsed at frequencies of 1, 2, 5, 10, and 20 Hz. The duration of a single pulse at each frequency was: 500 ms (1 Hz); 250 ms (2 Hz); 100 ms (5 Hz); 50 ms (10 Hz); and 25 ms (20 Hz), thus allowing the total duration of the stimulus (and odorant molecules encountering the moth), per second, to be the same. Each moth was individually tested to one of the odor frequencies, and used only once. Twenty to thirty moths were used for each frequency.

The second experimental series examined the effects of a background scent, or odorant, on the ability of the moth to track the *Datura* odor when it is pulsed at 1 Hz. Backgrounds used in these experiments included single volatiles, such as benzaldehyde (also in the *Datura* flower and creosote bush scents); geraniol (a monoterpene that is structurally similar to linalool, and important monoterpene in *Datura* scent in attracting moths); and ethyl sorbate (a volatile not in the *Datura* or creosote bush scents). Single volatiles allowed for testing how single olfactory "channels" modified the ability of the moths to track the *Datura* odor. Additionally, the background odors of creosote bush or the *Datura* odor were also used. Twenty to thirty moths were individually tested for each background treatment, and used only once.

The third experimental series examined the effects of toluene and xylene background on the ability of the moth to track the *Datura* odor (pulsed at 1 Hz). Background volatile concentrations used in these experiments were scaled to approximate the range of concentrations in the urban environment (2, 31-37). Twenty to forty moths were used in each experimental treatment.

In the natural environment, the moths may be exposed to the background odors for longer durations than those tested in the electrophysiological and behavioral experiments described above. Moreover, if the background volatiles were activating the same olfactory receptor cells as those responding to the *Datura* odor, then the prolonged exposure may cause adaptation and further decrease the ability of the moth's to locate the odor source. To test this, in the fourth experimental series we exposed moths to the background volatiles benzaldehyde, toluene, xylene, creosote bush scent, and the mineral oil control for 3 h before testing in the wind tunnel. After testing, moths for each treatment were placed in cages and their activity state (as measured by wing fanning) and mortality was assessed over a 24 h period. There were no significant differences in mortality between treatment groups (range: 3-7% mortality; Kruskal-Wallis test:  $P = 0.54$ ) or wing fanning responses (100% of moths could be induced to wing fan upon odor stimulation) indicating that the 3 h exposure did not adversely affect the moths.

The fifth and last series examined how inhibition in the moth antennal lobe influenced the ability for the moth to track and feed from the *Datura* odor source (see sections below for details on the drug delivery). Experimental treatment groups included 2 injection treatments and 3 odor stimuli, thereby creating a 2×3 experimental series. Drug treatments were saline-injected moths (injection control), and CGP54626 (GABA<sub>B</sub> receptor antagonist [50 μM])-injected moths. Moths were flown individually to the *Datura* odor pulsed at 1 Hz. In addition, to determine whether moths can navigate to an odor plume that was intermittent, a dynamic odor plume time series was created from the PTR-MS measurements of the *Datura* plume. The dynamic time series of odor pulses were tested on saline- and antagonist-injected moths. Last, a mineral oil (no odor) control for both injection treatments were tested to examine whether the injections modified the moth's casting and visuo-motor responses. Sixteen to twenty moths were used in each experimental treatment.

*Pharmacology and focal microinjection experiments:* To evaluate the contribution of inhibition in odor tracking behaviors of *Manduca* moths, a GABA<sub>B</sub> receptor antagonist (CGP54626; diluted in saline) was focal microinjected into the AL of 3 d old male moths. As a vehicle control, individual moths were injected with moth-saline. Moths were restrained in a plastic tube 30 min prior to scotophase and kept at room temperature in the light awaiting surgery and injection. Moths were de-scaled, the head capsule opened, and the ALs exposed and microinjected using a dual-channel Picopritzer (General Valve Corp, East Hanover, NJ). Injection was accomplished via Quartz pipettes (OD 1.0 mm, ID 0.70 mm, Sutter Instruments, San Diego, CA) pulled with a Model P-2000 laser puller (Sutter Instruments, San Diego, CA). Pipettes were manually inserted into the anterior region of each AL and 2 drops (mean diameter: 50 µm) were administered quickly in succession. After injection, the cuticle window was repositioned and sealed with myristic acid (Sigma) and the moth allowed to recuperate for 30 min before testing. We previously found that drugs delivered in this manner do not diffuse into other regions of the brain, and that the saline- and vehicle-injected moths behave not statistically different from non-injected moths (40).

### Electrophysiology

The total number of preparations in this study comprised 30 multichannel experiments (from as many moths; total units = 411), 16 EAG experiments (from as many moths), and 14 single sensillum recording experiments (from 8 moths).

Adult male *Manduca* were reared in the laboratory on an artificial diet (29) under a long-day (17/7 hr light/dark cycle) photoperiod and prepared for experiments 2–3 d after emergence (30, 41, 42). In preparation for recording, the moth was secured in a plastic tube with dental wax, leaving the head and antennae exposed. The head was opened to expose the brain, and the tube was fixed to a recording platform attached to the vibration–isolation table. The preparation was oriented so that both ALs faced upward, and the tracheae and sheath overlying one AL were carefully removed with a pair of fine forceps. The brain was superfused slowly with physiological saline solution (in mM: 150 NaCl, 3 CaCl<sub>2</sub>, 3 KCl, 10 N-tris[hydroxymethyl]methyl-2 aminoethanesulfonic acid buffer, and 25 sucrose, pH 6.9) throughout the experiment.

Olfactory stimuli were delivered to the preparation by pulses of air from a constant air stream were diverted through a glass syringe containing a piece of filter paper bearing the odor stimuli. The odor pulses were injected into a charcoal-filtered air stream flowing to the side of the antenna at a rate of 100 ml/min. The stimulus was pulsed by means of two solenoid-activated valve controlled by the TDT acquisition software (Tucker-Davis Technologies, Alachua, FL, USA). One solenoid valve was used to deliver the pulsed stimulus, whereas the second valve delivered the background. The outlet of the stimulus syringes were positioned 1 cm from and orthogonal to the center of the antennal flagellum ipsilateral to the AL of interest. Similar to olfactory stimuli tested in the wind tunnel experiments, the *Datura* odor was presented at different frequencies, from 1 to 20 Hz, with the duration of the pulse and the interpulse interval maintained constant. Background stimuli (benzaldehyde, geraniol, ethyl sorbate, toluene, and xylene) were presented for 5 sec (encompassing the duration of the pulsed stimuli). Concentrations were the same as those tested in the wind tunnel. In addition, to calibrate the recognition space for the *Datura* odor (detailed below), the three volatiles benzaldehyde, benzyl alcohol, and linalool were individually tested at the same concentrations as in the *Datura* odor. Last, the control solvent for the odors was mineral oil (no odor).

*Electroantennograms:* For EAG experiments, the antenna from a single male moth was cut and connected to two glass-electrodes filled with conductive gel. The EAG signal was recorded by Ag-AgCl wires and pre-amplified (10x) with a DAM50 (WPI, Sarasota, FL 34240) and connected to a RZ2 base station (Tucker-Davis Technologies, Alachua, FL, USA) and a RP2.1 real time processor (Tucker-Davis Technologies). The EAG signal was sampled at 400 Hz.

*Single sensillum recordings:* To determine whether olfactory receptor cells responded similarly to the different background mixtures (*Datura* and creosote bush scents) and single volatiles (benzaldehyde, benzyl alcohol, xylene, and toluene), single sensillum recordings were conducted to sample the responses of basiconic sensilla on the antennae of male *Manduca*. To eliminate movement of the antenna, the cibarial-pump muscles as well as the antenna muscle-bundles were removed with fine forceps. Dental wax was used to facilitate positioning and fixing the antenna on the recording platform. Recordings were made from the region on the dorsal surface of the antenna, near the leading edge of the annuli in the middle region of the antenna. The reference electrode was inserted into the distal end of the antenna and sealed with petroleum jelly to prevent desiccation. The glass (borosilicate) recording electrodes, pulled with a laser puller (P2000, Sutter Instrument, Novato, CA), were filled with sensillum lymph and connected to the headstage of an extracellular amplifier (1800, A-M Systems, Sequim, WA), to achieve 10,000× amplification. The signal was high-pass filtered and digitized at 20 kHz sampling rate. To gain electrical contact the recording electrodes were gently pressed against the sensilla, thereby gaining access to the interior of the targeted sensilla (20). Only sensilla that responded to aromatic volatiles (approximately 22% of the recorded basiconic sensilla) were used in the analysis.

*Ensemble recording and data analysis:* For recording the neural activity in the AL in response to the odor stimuli, we used a 16-channel silicon multielectrode recording array (a 4×4-3mm50-177; NeuroNexus Technologies, Ann Arbor, MI, USA) inserted into the moth AL. Extracellular activity was acquired with a RZ2 base station (Tucker-Davis Technologies, Alachua, FL, USA) and a RP2.1 real time processor (Tucker-Davis Technologies) and extracellular activity in the form of action potentials, or spikes, were extracted from the recorded signals and digitized at 25 kHz using the Tucker-Davis Technologies data-acquisition software (14, 30). Threshold and gain settings were adjusted independently for each channel, and spikes were captured in the 4-channel, or ‘tetrode’, recording configuration: any spike that passed threshold on one channel triggered the capture of spikes recorded on the other 3 channels on the same shank. Offline Sorter v.3 (Plexon Neurotechnology Research Systems, Dallas, TX, USA) was used to sort extracellular spikes based on their waveform shape (43), and spikes were assigned timestamps to create raster plots and calculate peri-stimulus time histograms (PSTH). The dimensions and spacing of the recording array make it possible to record stimulus-evoked neural activity from multiple sites across the AL.

To determine the ability of antennal responses or AL units to follow the odor pulses, we used a Pulse-Following-Index (PFI), which is based on the auto-correlograms (25). The peaks flanking the central peak on either side in the auto-correlograms are directly locked by odor pulses. Therefore,

$$\text{PFI} = C_{\text{ipi}} / \text{Sum}(C/n) \quad (1)$$

Where PFI represents pulse-following-index,  $ipi$  is the inter-pulse-interval (5 s for 0.2 Hz, 2 s for 0.5 Hz and so on),  $C_{ipi}$  is the correlation value at the specified  $ipi$  derived from correlograms,  $C$  is a vector of correlation values between the central peak (i.e. lag = 0) and the peak at  $ipi$ ,  $n$  represents the number of time bins between these two peaks. This ratio index reflects the contrast of spiking or electroantennogram activity between responses driven by odor pulses and the period between two adjacent responses. The better the antenna or neuron resolves odor pulses, the higher the PFI value is.

*Multivariate data analysis of population response:* Firing rate responses of neurons were binned for each unit into sequential 25 msec bins over a 5 sec (for 1 Hz stimulation – 500msec ON, 500msec OFF) or 1sec (for 5, 10, 20 Hz stimuli – equal duration of ON and OFF periods) interval from the onset of the stimulation. From the analysis we obtained unit firing rates matrix over time, such that the  $n$ -th row is the firing rate of the  $n$ -th unit. For the 1 Hz stimuli, we computed mean firing rate by averaging over 5 consecutive trials, with each trial is of 1 sec duration. Principal component analysis (PCA) was performed on the matrix of unit firing rate responses to compute population vectors for each stimulus. PCA was applied on a window of 200 msec during stimulation with each volatile constituent of the *Datura* odor (benzyl alcohol, benzaldehyde and linalool). For each volatile the most dominant principal component (vector with same number of elements as the number of units) was assigned as a unique population vector. In a similar manner we have computed a population vector that represents the *Datura* odor. To examine the dynamics of ensemble responses in the PCA coefficient space, firing rate responses to the *Datura* odor were projected onto the *Datura* population vector to provide a time series of the response dynamics (Figs. 3B<sub>2</sub>; S5). Similar projection was applied to the time series of firing rate responses to the *Datura* odor at different frequencies and embedded in different backgrounds (Figs. 3B<sub>2</sub>; S5, S6). For GABA-receptor antagonist (CGP54626) experiments, population response curves were obtained pre, during and post stages of the drug application (Fig. 4A<sub>2</sub>).

#### Analysis of odor classification: Recognition

*Odor space:* To further quantify differences in odor-evoked responses by the neural ensemble, we constructed an “odor space” from response vectors associated with the 3 volatiles comprising the *Datura* mixture. Each axis in this space corresponds to a volatile (benzyl alcohol, benzaldehyde and linalool) and the *Datura* odor is a vector within the axes of the 3 volatiles. To achieve representation of a distinct axis for each volatile, a transformation of the population vectors, obtained with PCA, was applied to obtain optimal orthogonal vectors. The transformation generates an orthogonal basis which incorporates a selective set of responsive neural units (*sensu* (18)). Construction of the odor space was verified by projecting the time series of stimulus-evoked responses, where each trajectory – representing the evolution of neural ensemble responses – to a given volatile stimulus projects to its cognate axis. When the stimulus is ON the trajectory is attracted to a fixed point located at the value of 1 on that axis (Figs. S6, S7). The *Datura* odor trajectory projected into the odor space appears as a combination of axes (Figs. 3C; S7). The fixed point of the *Datura* odor is defined by the region in the odor space where the *Datura* trajectory reaches a steady-state location during odor stimulation.

Projection of the *Datura* odor at different frequencies and backgrounds into the odor space allows us to compare how they differ from the trajectory of the *Datura* odor presented alone at the 1 Hz frequency. For example, when the neural ensemble population is stimulated with the *Datura* odor and benzaldehyde background, the trajectory of population vector responses orients toward the benzaldehyde axis. Moreover, higher frequencies of the *Datura* odor shrink the trajectory and rotate it to be in equal distance from all axes, similar to that which occurred when the neural ensemble was stimulated with the mineral oil (no-odor control) stimulus (Fig. 3C-E).

*Recognition:* Within the odor space, individual volatiles are represented by fixed points. Thus the odor space provides an optimal way in which to perform odor recognition tasks. Specifically, provided dynamical trajectories reach a prescribed neighborhood of the fixed point (e.g., a sphere or ellipsoid), then the odor is registered as a "recognition", or classification, of the input stimulus (Figs. 3C, D; S10; Tables S2, S3). Each time a dynamical trajectory enters the prescribed neighborhood of the fixed point (hereafter, 'recognition region') it is counted as evidence for the presence of the given stimulus. In particular, by computing the percentage of time (out of total stimulus application time) that the trajectory spent in a particular recognition region we can obtain an estimate of how the stimulus is associated with the corresponding odor. For example, the *Datura* stimulus is applied for 500 msec at a 1 Hz rate for 5 consecutive trials. To achieve a recognition score of 100% on a given trial, 50% of the trajectory points should reside in the recognition region that corresponds to the *Datura* odor fixed point. For each stimulus, the mean recognition and its standard deviation is calculated over 5 trials.

### Modeling odor classification and recognition

Theoretical and computational models of the olfaction stimulus processing in the AL can be of significant value to understanding the overall classification and recognition of odors. Moreover, they allow for detailed studies of parameter dependencies, sensitivity, and robustness which may be impractical or impossible to achieve in experiment due to limitations in recording and/or manipulation of the AL. For instance, a well-constructed model can ascertain the critical effects of varying levels of inhibition on the olfactory processing, thus illustrating the fundamental effects of a crucial biophysical process in the AL.

We use well established firing rate models for the interacting receptor neurons (RNs), local interneurons (LNs) and projection neurons (PNs) that participate in shaping the population vectors observed in experiment. The model introduces two aspects: an optimal odor space for describing the dynamics, and a data-driven strategy for prescribing a self-consistent connectome for the AL. These innovations in conjunction with a standard firing rate model provide an accurate predictive model for the dynamics of the AL during olfaction processing. As such, a careful study can be made of the role of inhibition in shaping the population vectors and performing odor classification. In such studies, decreasing inhibition is shown to lead to deleterious effects such as poor recognition of odors.

To determine how varying levels of inhibition affects odor recognition, we used a computational model that constructs an optimal neural network from the electrophysiological data (18). The construction uses the axes vectors of the odor space to calibrate interaction (i.e., synaptic connections) of local interneurons (LNs) with projection neurons (PNs) in the AL. The

interaction is expressed by lateral inhibition from LNs to PNs. Such interaction is known to be responsible for shaping the firing rate activity of PNs (17, 44, 45). The input into the computational model is the input into the AL, modeled as the input from olfactory receptors on the antenna. After calibration, the model is capable of simulating the firing rate dynamics of the AL neurons, and particularly of PNs as a response to other stimuli. The input can take a form of any combination of the volatiles. For more mathematical/technical details underlying model construction see (18). Briefly, we model the network of three vectors ( $\mathbf{x}$ ,  $\mathbf{y}$  and  $\mathbf{z}$ ) of firing rate units corresponding to the three anatomical groups of RNs, PNs and LNs respectively:

$$\dot{\mathbf{x}} = -\mathbf{x} + \mathbf{J}, \quad (2)$$

$$\dot{\mathbf{y}} = -\beta\mathbf{y} + [A\mathbf{x} - B\mathbf{z}]^+, \quad (3)$$

$$\dot{\mathbf{z}} = -\gamma\mathbf{z} + [C\mathbf{x} - E\mathbf{z}]^+, \quad (4).$$

The input into the PNs and LNs is modulated by a standard linear threshold function denoted by  $[ ]^+$  (46). The vector  $\mathbf{J}$  is the external input into the receptor cells on the antennae. The matrices  $A$ ,  $B$ ,  $C$  and  $E$ , which are not biophysically known, describe the interactions between the cells. The rows represent the output cells and the columns represent the input cells (Fig. S9).

Matrices  $A$  and  $C$  represent the input from RN cells to PN and LN cells, respectively, and are set as diagonal matrices (local input). The matrix  $B$  represents interaction directed from LN cells to PN cells, and  $E$  represents interaction within LN population (Fig. S9). To date, there is not enough biophysical information to construct these matrices, i.e., the connectome of the AL remains unsolved. We find the topology of the matrix  $B$  by assuming  $E$  as a random matrix.

To infer the topology of  $B$  we use population vectors of each volatile  $i$ , denoted by  $\mathbf{y}_i^P$ , derived from the electrophysiological recordings of PN neurons (18, 47). We describe how we obtained these vectors in ‘Multivariate data analysis of population response’ section. We then construct a library, the matrix  $O$ , from the population vectors. The columns of  $O$  (except the last one),  $\mathbf{o}_i^P$ , are the axis vectors of the ‘odor space’, i.e., orthogonal distinct vectors representing the population response per single volatile. Here these are three vectors that correspond to volatiles benzyl alcohol, benzaldehyde and linalool that constitute the *Datura* odor. The last column in  $O$ , the vector  $\mathbf{o}^R$ , is the remainder vector (sum of all other orthogonal directions to the axis vectors that do not represent any volatile).

$$L = \begin{bmatrix} \vdots & & \vdots \\ \mathbf{y}_1^P & \cdots & \mathbf{y}_l^P \\ \vdots & & \vdots \end{bmatrix}_{N \times l} \xrightarrow{U} O = \begin{bmatrix} \vdots & & \vdots & \vdots \\ \mathbf{o}_1^P & \cdots & \mathbf{o}_l^P & \mathbf{o}^R \\ \vdots & & \vdots & \vdots \end{bmatrix}_{N \times l+1}$$

where  $U$  represents the transform from the population vectors found from the electrophysiological recordings to the optimal odor space for individual volatiles. Projection of the PN dynamical equations, Eq. (3), onto the library vectors provides a division of these equations into two models: (i) A reduced model for the dynamics of population vectors, Eq. (5), where  $\mathbf{p}(t)$  is a vector of dynamical coefficients of the population vectors,  $\mathbf{J}$  is an external input vector into the RNs on the antennae and the vector  $\mathbf{J}^{\text{eff}}$  is the effective input contributed to each population vector, i.e. input into each volatile, and (ii) A model for the dynamics of remaining patterns.

$$\frac{d\mathbf{p}}{dt} = \tilde{M}\mathbf{p} + \mathbf{J}^{\text{eff}}$$

$$\tilde{M} = -\beta I, \mathbf{J}^{\text{eff}} = O^T(A - B\tilde{E}^{-1}C)\mathbf{J}_0. \quad (5)$$

Separating the system into two models, for population vectors and the remainder, allows us to impose constraints on the dynamics of each model individually. In particular, the remainder is expected to experience a rapid decay. However, the population vectors are expected to produce stable patterns of activity, i.e. they produce stable fixed points. To ensure these two model behaviors, we introduce a 4×4 weighting matrix  $W$  which ensures these two dynamical effects hold in the model. Thus  $W$  is picked to be consistent with experimental observations of the trajectory dynamics at 1Hz. Once determined, the only unknown in the model is the connectivity matrix  $B$  which can be found from the minimization problem:

$$\text{minimize } \|O^T(A - B\tilde{E}^{-1}C)\mathbf{J}_0 - W\|_{Fr},$$

where the minimization is performed using the Frobenius norm as denoted by the subscript,  $O^T$  is the transpose matrix  $O$ ,  $\tilde{E}$  is  $E + \gamma I$ ,  $\mathbf{J}_0$  is the matrix of external inputs with the vectors  $\mathbf{J}$  as columns. The minimization problem produces the matrix  $B$  that when paired with matrices  $A$ ,  $C$  and  $E$  provide a robust and accurate representation of the odor space dynamics directly observed in experiment. Thus our data-driven strategy produces a connectomic pairing between RNs, LNs and PNs cells that is consistent with experimental observation. Once the connectome is established, and unlike experiments, we can finely manipulate inhibition levels, for instance, to understand its deleterious impact on a classification task.

The validity of the model is verified with an input that corresponds to the *Datura* odor presented at 1 Hz: an equal ratio input of the 3 volatiles + random additive input of 20% (noise). Multiple simulations of the model produce odor space trajectories and recognition scores similar to empirical results from stimulation with the *Datura* odor presented at 1 Hz (Figure 4B, inhibition 100%).

With the synaptic connections calibrated and verified for the *Datura* odor input, we use the model to simulate the effect of reducing inhibition in the circuit. To simulate these effects, we keep the topology of the inhibitory connections fixed and vary gradually the inhibition amplitude parameter from 100% (calibrated) to 0% (inhibition is blocked) with steps of 10%. Simulating the model dynamics with the *Datura* odor input for 5s we compute the recognition scores associated with each inhibition amplitude value (Fig. 4B). Based on the simulations, we find that high levels of calibrated inhibition (90-100% amplitude levels) are necessary for the model to produce significant recognition scores above 50%. For example, the model trajectories for three different inhibition levels (100%, 50% and 0%) were examined and quantified in odor space demonstrating that global manipulation of inhibition alters the excursions of the *Datura* odor (Fig. S10). Moreover, as inhibition decreases, trajectory excursions become more random and do not settle to the zero fixed point within 1 s period (Fig. S10). Interestingly, the features of inhibition manipulated trajectories resemble the features of trajectories of *Datura* odor stimulus at higher frequencies and background volatiles that shift the trajectory in the odor space (e.g., benzaldehyde) (Figs. 3C; S10). Such analysis indicates that inhibition calibration and its full activation are critical for correct population responses.

## Pharmacology and multichannel recording experiment

To determine the effects of the GABA<sub>B</sub> receptor antagonist on AL neuronal responses, multi-channel experiments were conducted. This method provides stable, long-term (> 5 h), electrophysiological recording that permit pharmacological manipulations to be made to AL neurons (30), while permitting examination at the level of the ensemble (n = 12 preparations; 172 neural units). Similar to behavioral experiments described above, the antagonist was diluted in physiological saline solution to 50 μM and then applied to moth preparations. A drip system comprising multiple 60-cc syringes converging on a central Teflon tube was used to facilitate quick switching from normal physiological saline solution to antagonist solution and back. The odor-evoked responses were first recorded under the normal physiological saline solution and then repeated under antagonist diluted in normal saline solution, and finally the normal saline wash.

## Histological identification of recording locations

To examine the location of the multi-channel recording probes, prior to recording experiments the probes were dipped in fluorescent dye (Alexa 568 hydrazide; A-10437, Invitrogen) before the recordings. After successful experiments, brains were rinsed with moth-saline and the brain was excised and immersed in 2% glutaraldehyde in 0.1 M phosphate buffer. Brains were fixed for 12 h, then dehydrated with a graded ethanol series, cleared in methyl salicylate, and finally imaged as whole mounts with a laser-scanning confocal microscope (Zeiss 510 Meta equipped with a 457 nm argon laser). Optical sections at 5 μm reliably revealed the tracks of the four multi-channel shanks in the AL (Fig. S12). To examine consistency of the probe position in the AL, confocal image stacks were reconstructed and analyzed using Amira v.4.1.2 (Indeed-Visual Concepts, Houston TX, USA). The macrogglomerular complex (MGC) and the labial pit organ glomerulus (LPOG), a large glomerulus located in the anterior region of the AL, were used as landmarks to determine the location of the electrodes relative to the surrounding glomeruli and compare the placement of the electrodes between preparations. Glomerular structures in the AL were labeled as previously described (13, 14, 30). Three-dimensional reconstructions of the impaled and neighboring glomeruli demonstrated the consistency between preparations on the location of the recording sites.

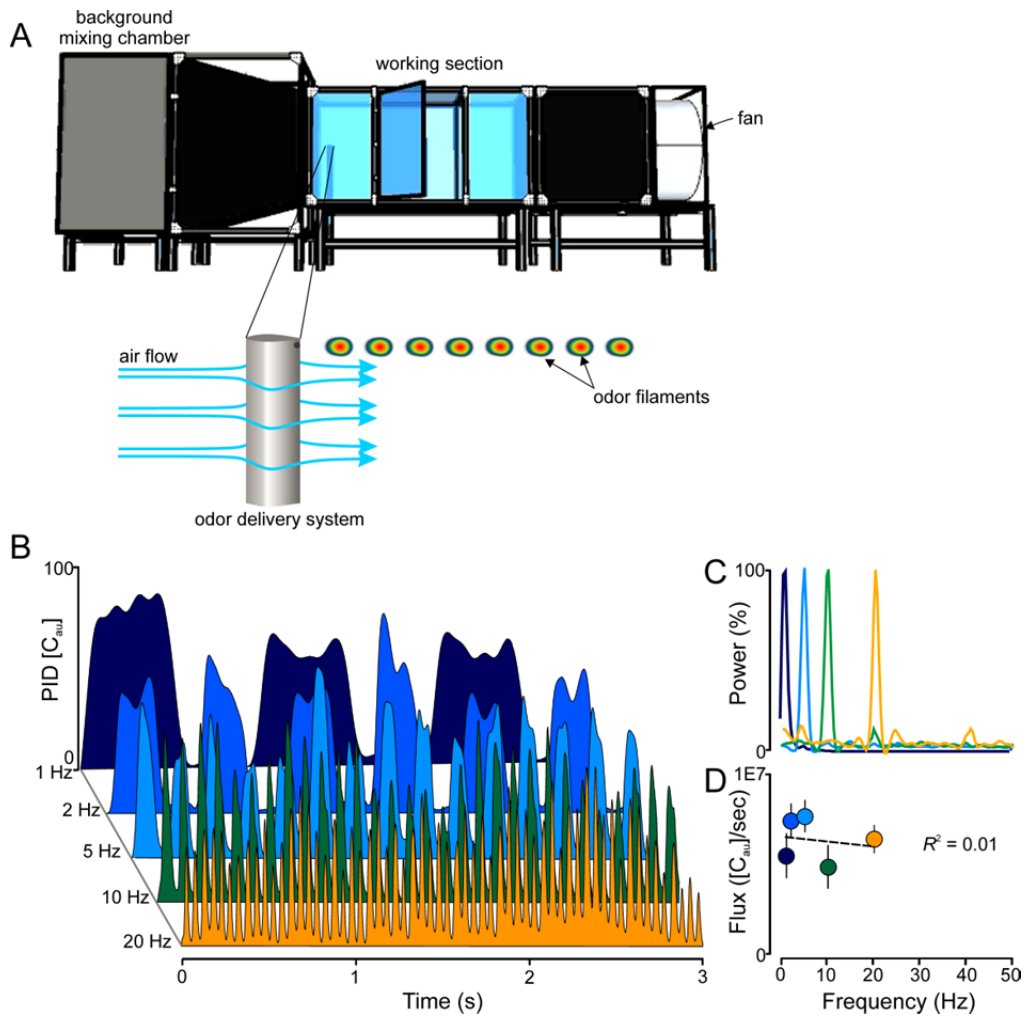


**Fig. S1.** (A) Experiments were performed in a  $2.5 \times 1.0 \times 1.0 \text{ m}^3$  wind tunnel (A, *top*), equipped with a camera-based 3D tracking system to observe moths as they navigate to the pulsed plume. Odors were delivered isokinetically by a computer-controlled solenoid system that emitted the odors from an airfoil that minimized disturbance to the flow of air (0.5 m/sec. wind) (A, *bottom*). (B) Time series of odor pulses (1 to 20 Hz) as measured by a photoionization detector (200B miniPID; Aurora Scientific, Aurora, Ontario CA). (C) Frequency spectrum of concentration changes at four different pulse frequencies: 1, 5, 10 and 20 Hz. Each trace is the mean of three 2-min. recordings at 300 Hz. (D) Flux, or concentration of odor molecules (as measure by PID  $[C_{\text{au}}]$ ) per sec. ( $[C_{\text{au}}]/\text{s}$ ), for each frequency. The flux at each frequency was not significantly different (one-way ANOVA:  $F_{4,15} = 2.19$ ,  $P = 0.14$ ); this was also reflected in the linear regression ( $R^2 = 0.01$ ;  $F_{1,15} = 0.20$ ,  $P = 0.65$ ). Symbols are the Mean  $\pm$  SEM; the dashed line is the linear regression.

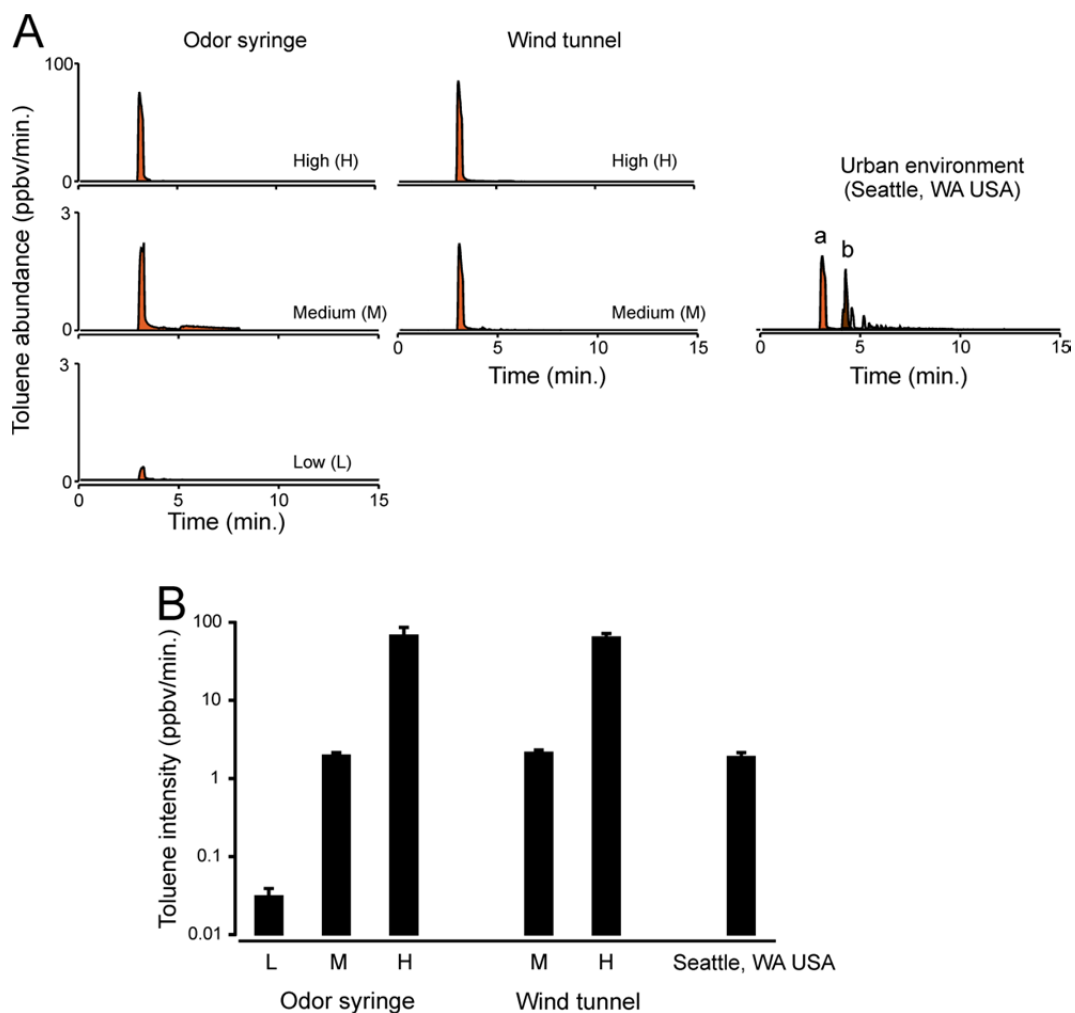


**Fig. S2.** Toluene in the odor syringes and wind tunnel were scaled to the range of those measured in the environment. (A, *left*) Ion chromatograms of toluene (light brown peak) at three intensities in the odor syringes (High [H]; Medium [M]; and Low [L]); (A, *middle*) two intensities in the wind tunnel (High and Medium intensities); (A, *right*) and measured in Seattle WA USA (47° 39.677', -122° 18.712') during two days in 2013 (December 10 and 11; 08:00-09:00 both days; temperatures ranged from 1.1 to 5.5 °C ). Peak labels for the Seattle chromatogram correspond to toluene (a) and p-xylene (b). (B) Emission rates of toluene.

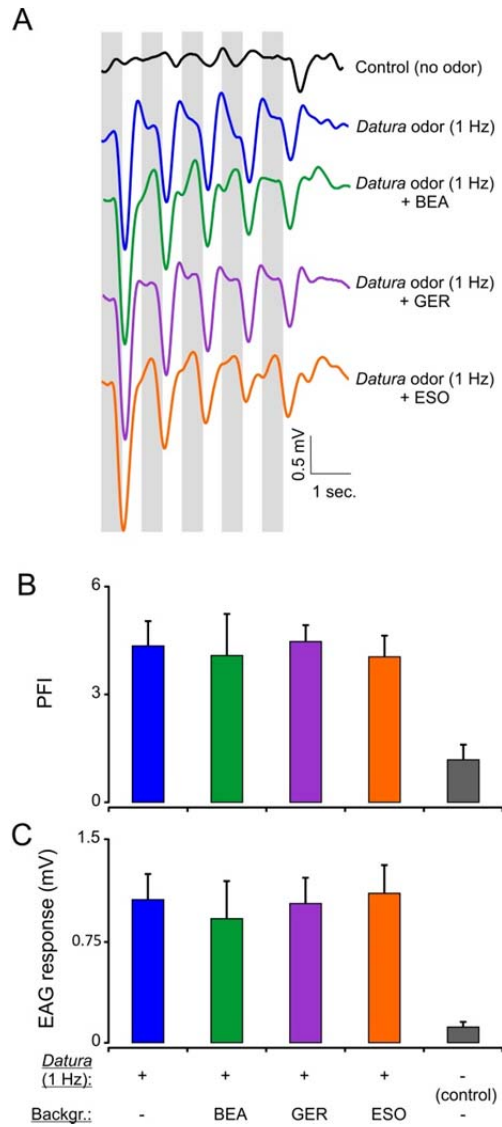


**Fig. S3.** Antennal (EAG) responses to 1 Hz pulses of the *Datura* odor in the presence of different volatile backgrounds. (A) EAG traces to five 1 Hz pulses of *Datura* odor in the presence of benzaldehyde (BEA; green), geraniol (GER; purple), or ethyl sorbate (ESO; orange) backgrounds. Mean PFI (B) and EAG (C) responses to the *Datura* odor embedded in different backgrounds. For both PFI and EAG responses, there are no significant differences between the *Datura* odor alone in comparison to the odor embedded in the different backgrounds (repeated measures ANOVA with Tukey post-hoc test:  $P > 0.90$ ). Bars are the mean  $\pm$  SEM.

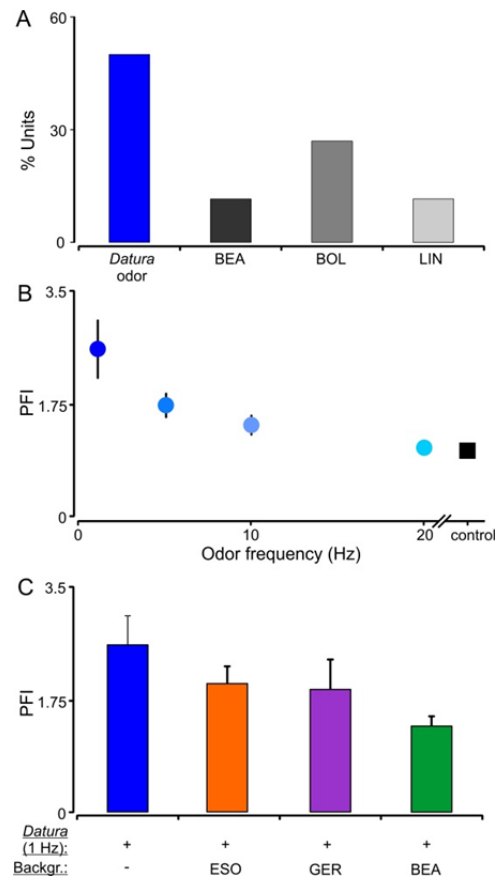


**Fig. S4.** Responses of AL neurons to the *Datura* odor at different frequencies and embedded in different backgrounds. **(A)** Percentage of neurons that best tracked the different odor stimuli; that include the *Datura* odor and the constituents of the *Datura* odor (benzaldehyde [BEA]; benzyl alcohol [BOL]; and linalool [LIN]). **(B)** Pulse Following Indices (PFI) for AL neurons in response to the *Datura* odor presented at different frequencies. **(C)** PFIs for AL neurons in response to the *Datura* odor embedded in different volatile backgrounds.

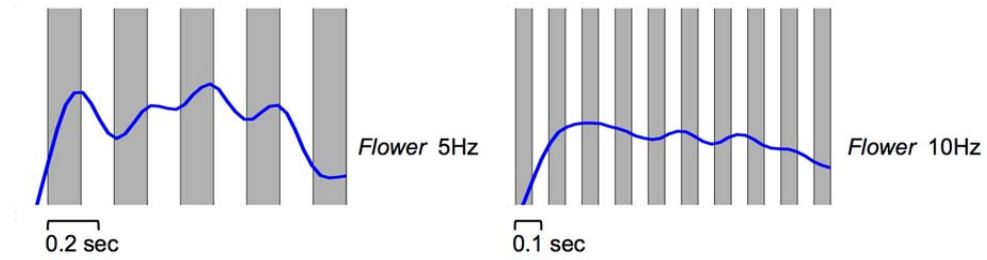


**Fig. S5.** Population responses (coefficient plots) to the *Datura* odor stimulus with varying frequencies (*left*: 5 Hz and *right*: 10 Hz) over duration of 1s (supplementary to Figure 3B<sub>2</sub>).

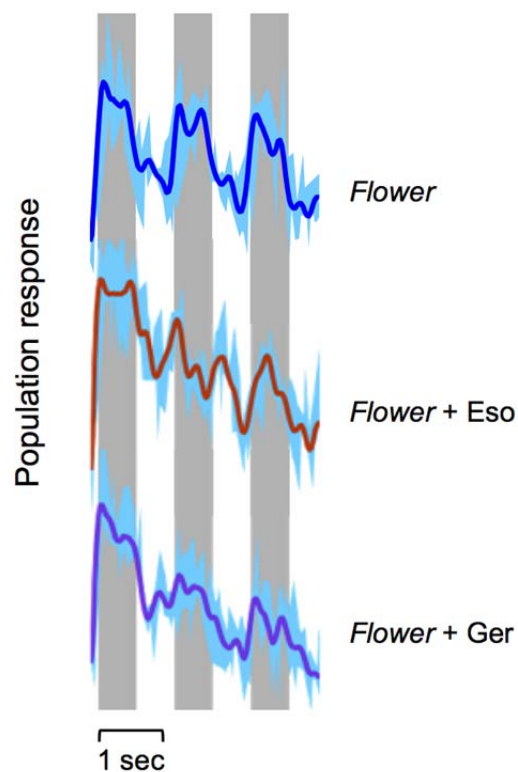


**Fig. S6.** Population responses (coefficient plots) supplementary to Figure 3B<sub>2</sub> (duration of 3s). *Top:* Population response (bold line, blue) to the *Datura* odor stimulus through time. The response is time-locked to the stimulus pulses (gray bars) and the peaks of the response all pass the value of 1. *Middle, bottom:* Population responses to the *Datura* odor embedded in background volatiles ethyl sorbate (ESO; orange line), and geraniol (GER; purple line). The mean responses are less correlated with stimuli pulses within each trial. In several trials the response did not exceed the value of 1. In all experiments from trial to trial the magnitude of the peak of the population mean is decreasing due to dilution of the odor. For visualization, the mean was smoothed with Gaussian filter (displayed as bold). Areas around the line represent the standard deviation from the mean.

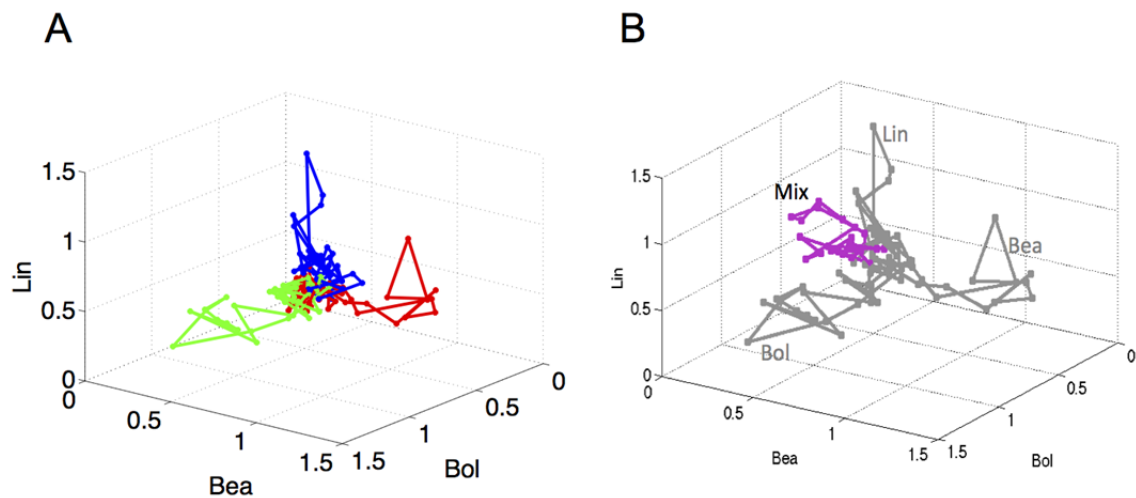


**Fig. S7.** Odor space construction and dynamic trajectories of the population vectors. Each axis is a population vector that corresponds to one of the three odorants benzaldehyde (BEA), benzyl alcohol (BOL) and linalool (LIN). **(A)** Average trajectories obtained from projecting the response time series of each stimulus (red: BEA, green: BOL, blue: LIN) show that the construction produces an optimal orthogonal space. **(B)** The *Datura* odor trajectory in odor space (purple) along with the volatile (gray) trajectories. The *Datura* odor trajectory is a combination of the three axes (volatiles). With the *Datura* trajectory we can identify the *Datura* odor fixed point, or the region in the odor space to which the trajectory is attracted.

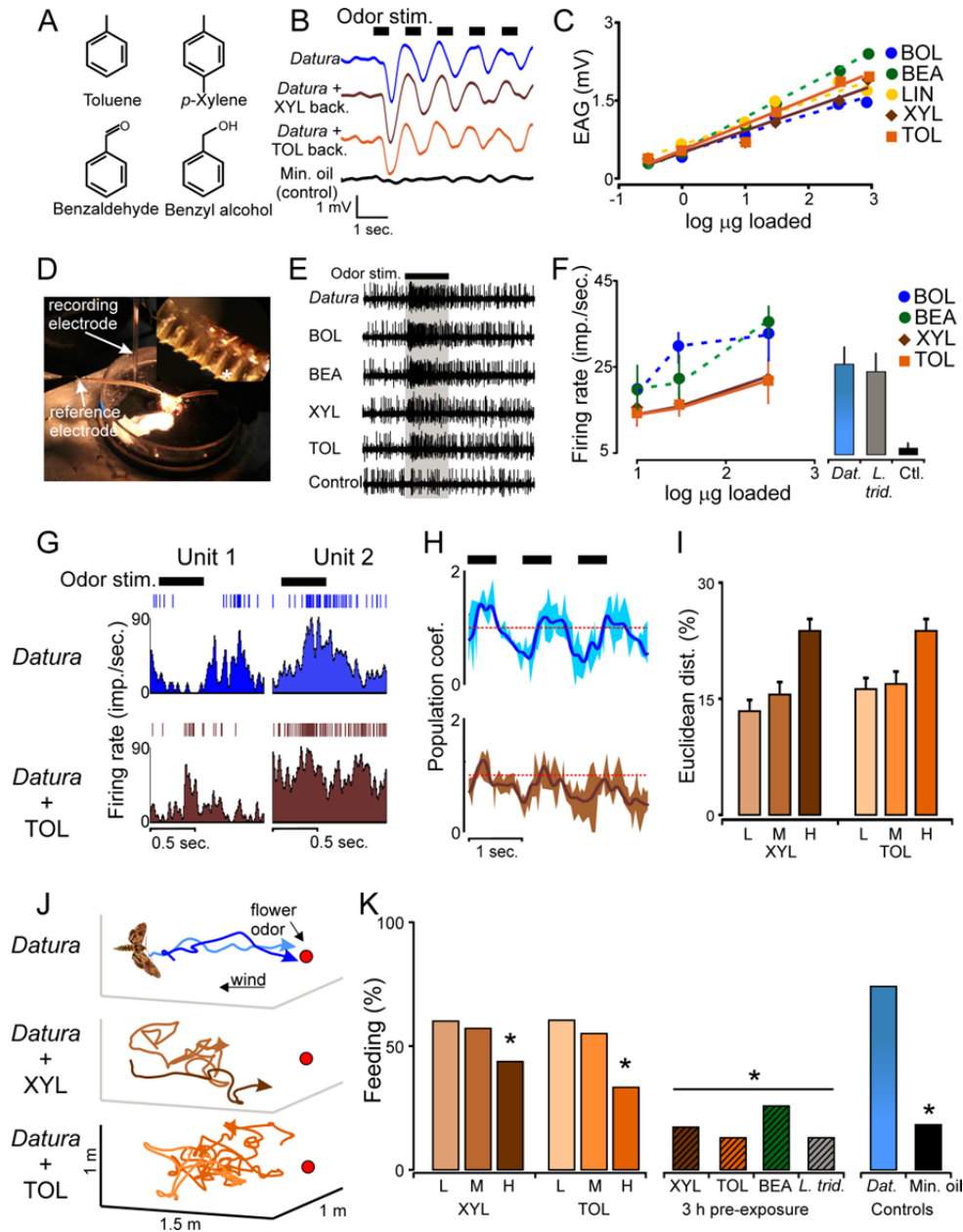


**Fig. S8.** Stimulation with toluene and *p*-xylene affects the balance of excitation and inhibition in the moth AL and decreases behavior. (A) Chemical structure of the volatiles toluene (TOL), *p*-xylene (XYL), benzaldehyde (BEA), and benzyl alcohol (BOL); the latter two volatiles are in the *Datura* odor. (B) EAG responses to pulses of the *Datura* odor either alone or embedded in the backgrounds of TOL or XYL. The TOL and XYL backgrounds did not affect the pulse-following responses of the antenna. (C) XYL and TOL elicited similar EAG responses as the constituents of the *Datura* odor: BEA, BOL and LIN (repeated measures ANOVA with Tukey post-hoc test:  $P > 0.93$ ). (D) Single sensillum recordings (SSR) were conducted to determine if XYL and TOL elicited responses in the same olfactory receptor cells that responded to BEA and BOL. SSRs were conducted in the basiconic sensilla of male *Manduca*. (E) Responses of a sensillum to the different olfactory stimuli. (F) Mean firing rate responses from 14 olfactory receptor cells (ORCs) to single volatiles at different intensities (scatter plot, *left*) and the *Datura*

(*Dat.*) and creosote bush (*L. trid.*) odors (histograms, *right*). Although ORC responses to the different odor stimuli were significantly greater than the mineral oil (no odor) control (Kruskal-Wallis test with multiple comparisons:  $\chi^2 = 40.67$ ;  $P < 0.05$ ), responses were not significantly different between odor stimuli (multiple comparisons:  $P > 0.05$ ). Plotted is the Mean  $\pm$  SEM firing rate response for each stimulus. **(G)** Multichannel recording responses of AL neurons in response to the *Datura* odor embedded in the TOL and XYL backgrounds at different intensities. The response of two neurons to the *Datura* odor (blue histograms and rasters) and the *Datura* odor embedded in the TOL background (brown histograms and rasters). **(H)** Population-level responses of AL neurons to three sequential pulses of the *Datura* odor alone (blue) and *Datura*+TOL (brown). Thick line is the mean; shaded area denotes the standard deviation. **(I)** Euclidean distance of the *Datura* odor embedded in the TOL and XYL backgrounds at different intensities (L is 2.3 ppb; M is 118 ppb; and H is 4059 ppb; *Datura* odor alone is the origin). Bars are the mean  $\pm$  SEM (8 preparations;  $N = 86$  units). **(J)** 3D flight tracks of moths navigating to plumes in different olfactory backgrounds: *Datura* odor alone (*top*, blue tracks); *Datura*+XYL (*middle*, brown tracks); and *Datura*+TOL (*bottom*, orange tracks). **(K)** Percentage of moths that successfully navigated to, and attempted to feed from, the odor source ( $N = 20$ -40 moths per treatment).

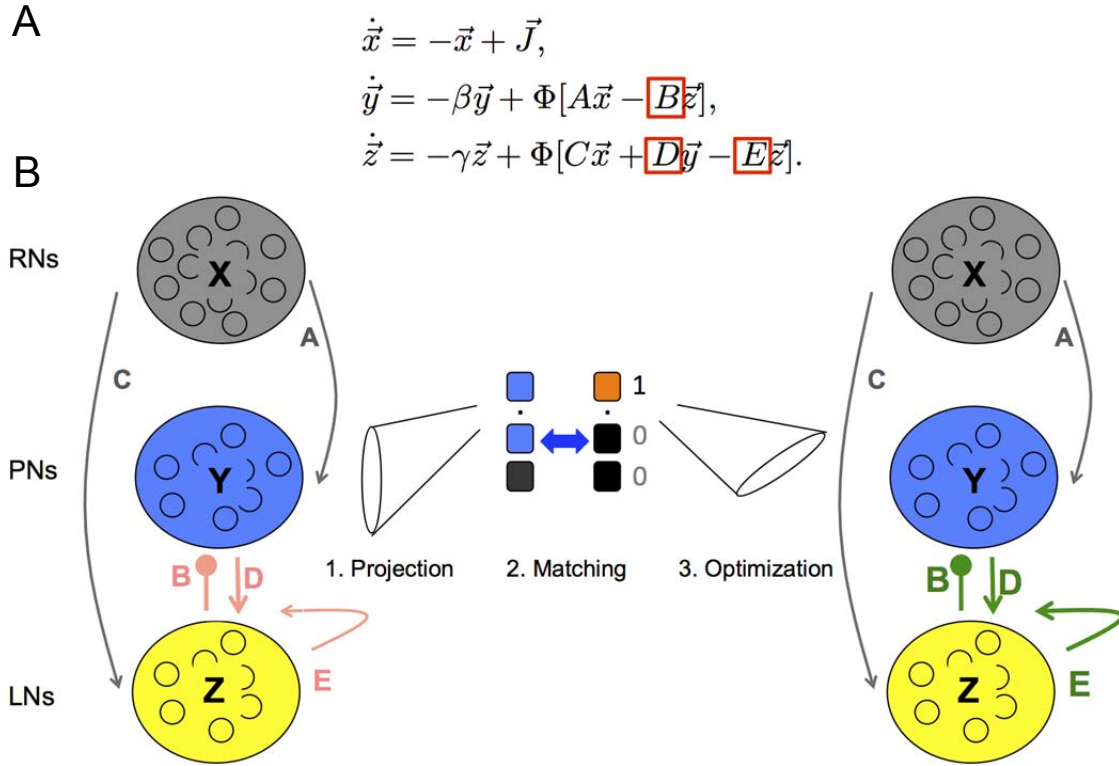


**Fig. S9.** Construction of a computational model for the AL dynamics. **(A)** We model the response dynamics of the neurons belonging to populations RNs ( $x$ ), PNs ( $y$ ), and LNs ( $z$ ) with a standard firing-rate model where  $\Phi$  is a linear function with a threshold (27). The matrices  $A$ ,  $B$ ,  $C$ ,  $D$  and  $E$  denote the connectivity matrices between the firing rate units within the populations. The matrices marked in red (connectivity of PNs and LNs) are to be calibrated. **(B)** Calibration of the model. We use the population vectors (axes of the odor space) obtained from the recorded data to project the implicit equations (with unknown connectivity matrices) to obtain a low dimensional model for the dynamics of the population vectors. The low-dimensional model is then restricted to have a unique fixed point at 1 on the corresponding axis to a given volatile stimulus. We then use a convex optimization to recover a plausible setup of connections that support these dynamics.

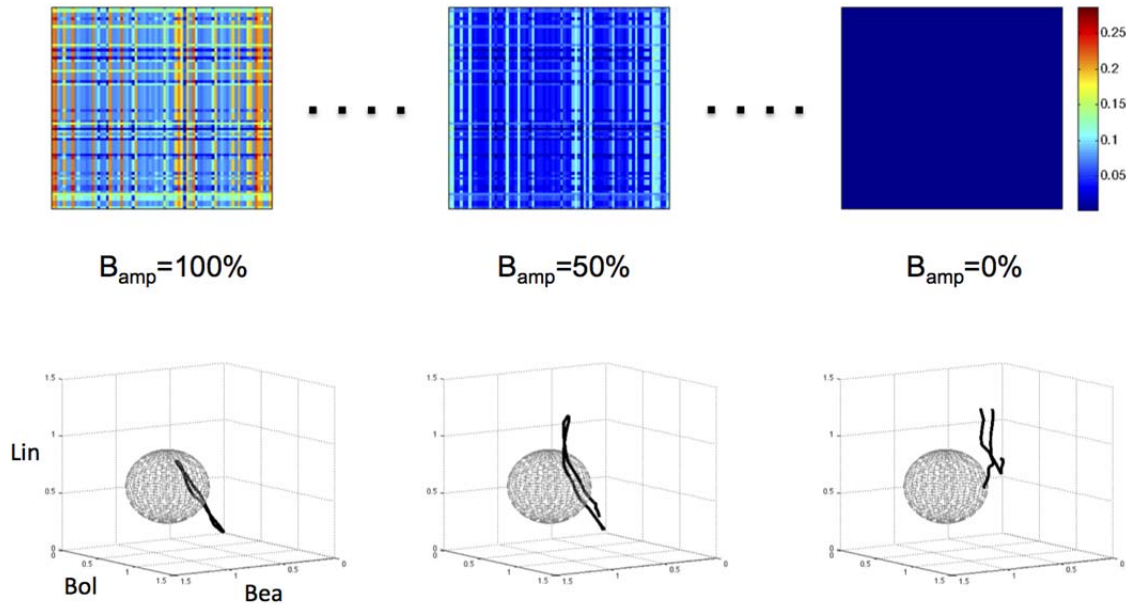


**Fig. S10.** The effect of varying the inhibition amplitude,  $B_{amp}$ , in the model. From left to right we vary the LNs inhibition of PNs, i.e. the coefficient that multiplies the connectivity matrix  $B$ , from calibrated value (100%) to no-inhibition (0%) with steps of 10%. *Top row:* Color plots of the elements in the matrix  $B$  for  $B_{amp} = 100\%$ , 50% and 0%. *Bottom row:* Corresponding resultant model trajectories projected into the odor space. Along with the trajectory we show the recognition region in the odor space associated with the *Datura* odor. For  $B_{amp} = 100\%$  the trajectory starts from zero (meaning that it was able to return to it in the 1<sup>st</sup> trial) and enters the recognition region. The trajectory spends approximately 435 msec in the recognition region out of the 500 msec application time of the stimulus. The trajectory returns back to zero when the 1s has been lapsed. For  $B_{amp} = 50\%$ , the trajectory initiated away from zero as well. The course of the trajectory is shifted in comparison to the trajectory for 100%. It appears to be more tangent to the recognition region and intersects it only for a small amount of time, less than 50ms. The trajectory does not return back to zero within the period of 1 s of the second trial. For  $B_{amp} = 0\%$ , the trajectory is initiated away zero near the values of 0.5 in all axes. The trajectory is noisy (stochastic) and is not attracted to the *Datura* odor recognition region. After 1 sec, the trajectory does not return back to zero or the initiation point.

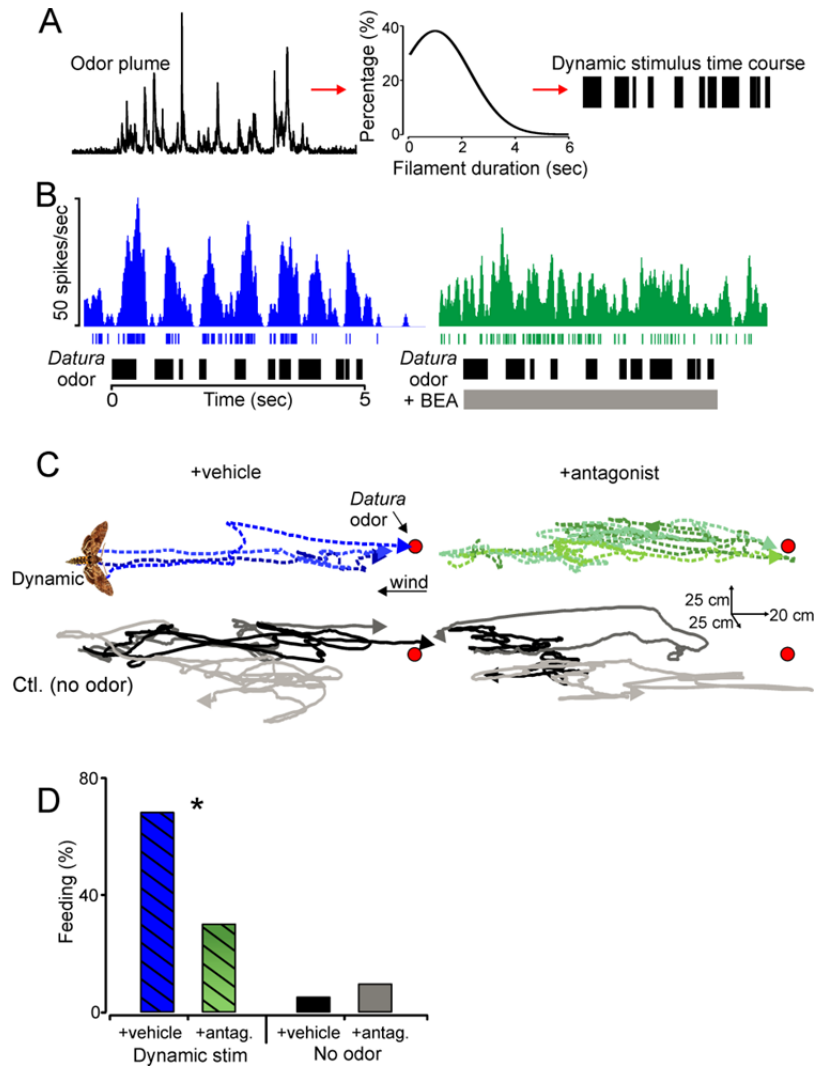


**Fig. S11.** The effects of inhibition in encoding a naturalistic, temporally dynamic, odor plume. (A) To simulate the temporal dynamics of an odor plume (A, *left*), the frequency distribution of odor-laden filaments was determined for an odor plume measured in the field (A, *middle*). Based on this distribution, a stimulus time course, represented as black bars, was constructed from the distribution (A, *right*). (B) PSTH of single neuron responses to the *Datura* odor (*right*) and the *Datura* odor + BEA background. Bars plotted below the PSTHs and rasters are the period of the dynamic stimulus. (C) Flight tracks of saline- (+vehicle) and antagonist-injected (CGP54626; +antagonist) moths in the wind-tunnel. Using *Datura* odor as the source, the vehicle-injected moths flew directly toward the dynamic odor source (*left*, dashed blue lines), thus resulting in approximately straight flight tracks. Antagonist-injected moths had more tortuous trajectories to the dynamically-pulsed *Datura* odor source (*right*, dashed green lines). Similar results were obtained when these two treatment groups were flown to the 1 Hz *Datura* odor stimulus (Fig. 4C, D). Replacing the *Datura* odor with the no-odor (mineral oil) control in the wind-tunnel resulted in cross-wind casting in these moths (*bottom*, grey lines). (F) Percentage of moths that attempted to feed from the odor source. Asterisks denote a significant difference between vehicle- (dashed blue bars) and antagonist-injected (dashed green bars) moths ( $2 \times 2 \chi^2$ -test:  $P < 0.05$ ). Each bar represents 20-30 moths.

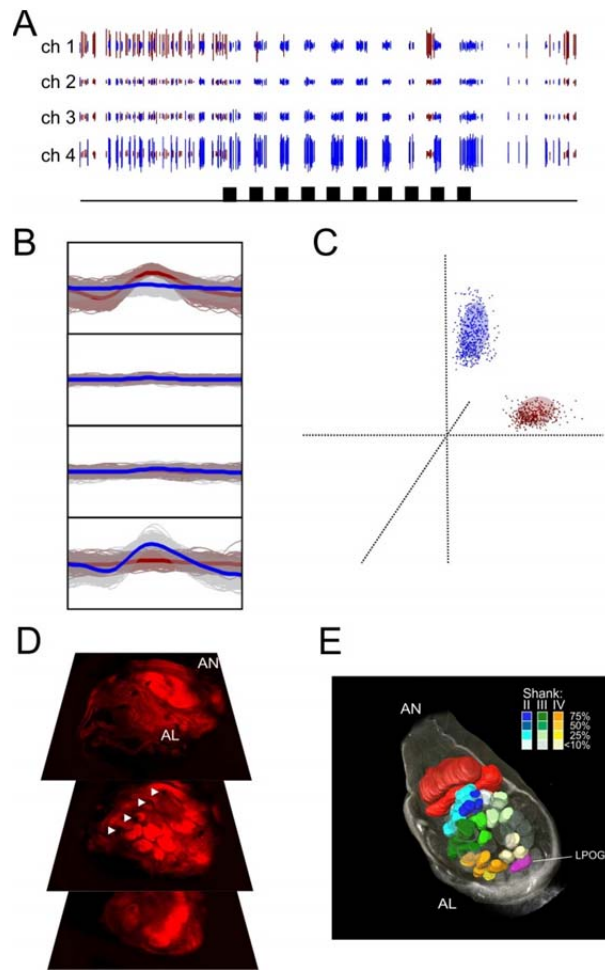


**Fig. S12.** Spike-sorting of tetrode recordings and recording positions. **(A)** Ten-pulse stimulation (1 Hz) with the *Datura* odor (black bars). Responses are shown for channels 1-4 for two units, red and blue. **(B)** The sorted units show different spike shapes on the tetrode recording channels. **(C)** The spike shapes cluster distinctly after principal components analysis, and are distinct from one another as shown by the shaded area (3.5 SD). **(D)** The four shanks of the recording probe are spaced such that the array encompasses a large volume of the AL thereby allowing the positioning of the four channels on each shank provided recording of broad zones within processing glomeruli and neuropil. White arrow heads denote tracks from the four shanks. **(E)** Blue glomeruli correspond to shank II, green for shank III, and yellow for shank IV. Shank I was placed in the MGC-T1 (MGC shown in red). The position of the probe was consistent between preparations. The color scale denotes the frequency that glomeruli were impaled or adjacent to the shanks for all preparations, e.g., deep blue glomeruli correspond to those glomeruli being impaled by shank II 75% of the time. Antennal nerve (AN); antennal lobe (AL); labial pit organ glomerulus (LPOG).

**Table S1.** Wind conditions at SRER field site

Velocity (m/s)			Turbulent intensity			Reynolds shear stress
$\bar{u}$	$\bar{v}$	$\bar{w}$	$I_u$	$I_v$	$I_w$	
0.57 (0.29)	0.16 (0.42)	0.10 (0.09)	0.17 (0.05)	0.21 (0.15)	0.09 (0.02)	0.07 (0.06)

**Table S2.** Recognition scores for varying frequency of the *Datura* odor

Stimulus freq.:	Recognition (%)	Correlation with the stimulus (%)
1 Hz	80	70.84
5 Hz	55	21.68
10 Hz	15	10.86
20 Hz	11	6.89

**Table S3.** Recognition scores for volatile backgrounds when the *Datura* odor is presented at 1 Hz.

Background:	Mean Recognition (%)	Standard deviation (%)
- ( <i>Datura</i> odor only; no background)	71.25	16.89
Ethyl sorbate	78.75	12.96
Geraniol	37.5	29.65
Benzaldehyde	12.5	12.5
Ctl (no <i>Datura</i> odor; no background)	0	0

## Supplementary Online Information – References

23. R. Alarcón, G. Davidowitz, J. L. Bronstein, Nectar usage in a southern Arizona hawkmoth community. *Ecol. Entomol.* **33**, 503-509 (2008).
24. S. A. Kurc, L. M. Benton, Digital image-derived greenness links deep soil moisture to carbon uptake in a creosotebush-dominated shrubland. *J. Arid. Environ.* **74**, 585-594 (2010).
25. J. de Gouw, C. Warneke, Measurements of volatile organic compounds in the earth's atmosphere using proton-transfer-reaction mass spectrometry. *Mass Spectrom. Rev.* **26**, 223-257 (2007).
26. W. Lindinger, A. Hansel, Analysis of trace gases at ppb levels by proton transfer reaction mass spectrometry (PTR-MS). *Plasma Sources Sci. T.* **6**, 111 (1997).
27. S. Hayward, C. N. Hewitt, J. H. Sartin, S. M. Owen, Performance characteristics and applications of a Proton Transfer Reaction-Mass Spectrometer for measuring volatile organic compounds in ambient air. *Environ. Sci. T.* **36**, 1554-1560 (2002/04/01, 2002).
28. R. A. Raguso, O. Pellmyr, Dynamic headspace analysis of floral volatiles: a comparison of methods. *Oikos* **81**, 238-254 (1998).
29. R. A. Bell, F. G. Joachim, Techniques for rearing laboratory colonies of tobacco hornworms and pink ballworms. *Ann. Entomol. Soc. Am.* **69**, 365-373 (1976).
30. J. A. Riffell, H. Lei, J. G. Hildebrand, Neural correlates of behavior in the moth *Manduca sexta* in response to complex odors. *Proc. Natl. Acad. Sci. U.S.A.* **106**, 19219-19226 (2009).
31. M. A. K. Khalil, R. A. Rasmussen, Forest hydrocarbon emissions: relationships between fluxes and ambient concentrations. *J. Air Waste MA.* **42**, 810-813 (1992).
32. C. Chan, J. D. Spengler, H. Özkaynak, M. Lefkopoulou, Commuter exposures to VOCs in Boston, Massachusetts. *J. Air Waste MA.* **41**, 1594-1600 (1991).
33. G. F. Evans, T. A. Lumpkin, D. L. Smith, M. C. Somerville, Measurements of VOCs from the TAMS Network. *J. Air Waste MA.* **42**, 1319-1323 (1992).
34. T. J. Kelly, P. J. Callahan, J. Pleil, G. F. Evans, Method development and field measurements for polar volatile organic compounds in ambient air. *Environ. Sci. T.* **27**, 1146-1153 (1993).
35. D. D. Parrish *et al.*, Internal consistency tests for evaluation of measurements of anthropogenic hydrocarbons in the troposphere. *J. Geophys. Res.-Atmos.* **103**, 22339-22359 (1998).
36. M. Chen, S. Chen, B. Guo, I. F. Mao, Relationship between environmental exposure to toluene, xylene and ethylbenzene and the expired breath concentrations for gasoline service workers. *J. Environ. Monitor.* **4**, 562-566 (2002).
37. J. F. Periago, C. Prado, Evolution of occupational exposure to environmental levels of aromatic hydrocarbons in service stations. *Ann. Occup. Hyg.* **49**, 233-240 (2005).
38. J. Pawliszyn, *Solid phase microextraction: theory and practice.* (Wiley-VCH Inc., New York, 1997).
39. S. Tumbiolo, J. Gal, P. Maria, O. Zerbinati, Determination of benzene, toluene, ethylbenzene and xylenes in air by solid phase micro-extraction/gas chromatography/mass spectrometry. *Anal. Bioanal. Chem.* **380**, 824-830 (2004).
40. H. Lei, J. Riffell, S. Gage, J. Hildebrand, Contrast enhancement of stimulus intermittency in a primary olfactory network and its behavioral significance. *J. Biol.* **8**, 21 (2009).

41. H. Lei, T. A. Christensen, J. G. Hildebrand, Spatial and temporal organization of ensemble representations for different odor classes in the moth antennal lobe. *J. Neurosci.* **24**, 11108-11119 (2004).
42. C. E. Reisenman, T. A. Christensen, J. G. Hildebrand, Chemosensory selectivity of output neurons innervating an identified, sexually isomorphic olfactory glomerulus. *J. Neurosci.* **25**, 8017-8026 (2005).
43. C. M. Gray, P. E. Maldonado, M. Wilson, B. McNaughton, Tetrodes markedly improve the reliability and yield of multiple single-unit isolation from multi-unit recordings in cat striate cortex. *J. Neurosci. Method.* **63**, 43-54 (1995).
44. T. A. Christensen, J. G. Hildebrand, Coincident stimulation with pheromone components improves temporal pattern resolution in central olfactory neurons. *J. Neurophysiol.* **77**, 775-781 (1997).
45. T. A. Christensen, B. R. Waldrop, I. D. Harrow, J. G. Hildebrand, Local interneurons and information processing in the olfactory glomeruli of the moth *Manduca sexta*. *J. Comp. Physiol. A.* **173**, 385-399 (1993).
46. C. Linster, S. Sachse, C. G. Galizia, Computational modeling suggests that response properties rather than spatial position determine connectivity between olfactory glomeruli. *J. Neurophysiol.* **93**, 3410-3417 (2005).
47. H. Lei, C. E. Reisenman, C. H. Wilson, P. Gabbur, J. G. Hildebrand, Spiking patterns and their functional implications in the antennal lobe of the tobacco hornworm *Manduca sexta*. *PloS one* **6**, e23382 (2011).